Supplementary Data for

Structural Basis of Protein Arginine Methyltransferase Activation by a Catalytically Dead Homolog (Prozyme)

Hideharu Hashimoto,[1] Lucie Kafková,[2] Ashleigh Raczkowski[3], Kelsey D. Jordan,[3] Laurie K. Read,[2] and Erik W. Debler[1]

1. Department of Biochemistry and Molecular Biology, Thomas Jefferson University, Philadelphia, PA 19107, USA
2. Department of Microbiology and Immunology, and Immunology and Witebsky Center for Microbial Pathogenesis and Immunology, SUNY Buffalo, Buffalo, NY 14203, USA
3. Simons Electron Microscopy Center, New York Structural Biology Center, New York, NY 10027, USA

Running title: *Trypanosoma brucei* PRMT1 enzyme prozyme structure

Correspondence to Erik W. Debler: Erik.Debler@jefferson.edu.
DOI: https://doi.org/10.1016/j.jmb.2019.11.002

This PDF file includes:

Supplemental Tables S1 and S2
Supplemental Figs. S1 to S7

Supplemental Table S1. Data collection and refinement statistics.

Data collection	
Beamline	NE-CAT 24-ID-C (APS)
Space group	C2
Cell dimensions	
a, b, c (Å)	a=196.6, b=65.9, c=141.0
α, β, γ (°)	α=γ=90, β=106.9
Wavelength (Å)	0.9792
Resolution (Å) [a]	50.0-2.40 (2.49-2.40)
No. of unique reflections	62,179 (3,760)
R_{merge} (%) [a,b]	7.4 (70.6)
CC1/2 [a]	0.997 (0.673)
CC* [a]	0.999 (0.897)
$\langle I / \sigma I \rangle$ [c]	24.0 (1.6)
Completeness (%) [a]	88.8 (54.0)
Redundancy [b]	7.3 (3.4)
Refinement	
Resolution (Å)	50.0 – 2.40
No. of reflections	55,457
Test set	1999
R_{work} [d]/ R_{free} [e] (%)	19.0 / 22.3
No. of atoms	10,318
R.m.s. deviations	
Bond lengths (Å)	0.003
Bond angles (°)	0.6
<B-Value> (Å^2)	
Protein	46.0
AdoHcy	46.3
MolProbity Score/Percentile	1.26/100th
Ramachandran plot [f]	
Favored (%)	97.0
Allowed (%)	3.0
Outliers (%)	0.0

[a]Highest-resolution shell is shown in parentheses.
[b]$R_{merge} = \Sigma \mid I - \langle I \rangle \mid / \Sigma I$, where I is the observed intensity and $\langle I \rangle$ is the averaged intensity from multiple observations.
[c]$\langle I/\sigma I \rangle$ = averaged ratio of the intensity (I) to the error of the intensity (σI).
[d]$R_{work} = \Sigma \mid F_{obs} - F_{cal} \mid / \Sigma \mid F_{obs} \mid$, where F_{obs} and F_{cal} are the observed and calculated structure factors, respectively.
[e]R_{free} was calculated using a randomly chosen subset (5%) of the reflections not used in refinement.
[f]As determined by MolProbity.

Supplemental Table S2. Comparison of *Tb*PRMT1 ENZ with other PRMTs.

	PDB accession code	Sequence identity	Rmsd (Å)	No. of Cα atoms
*Rn*PRMT1[a]	**1OR8**	51%	1.0	312
*Sc*RMT1[b]	**1G6Q**	47%	1.2	308
*Rn*PRMT3[a]	**1F3L**	41%	1.3	308
*Mm*CARM1[c]	**2V74**	35%	1.6	302
*Tb*PRMT1 PRO [d]	**6DNZ** (This study)	24%	2.1	293

[a]*Rn*: *Rattus norvegicus* (rat)
[b]*Sc*: *Saccharomyces cerevisiae* (budding yeast)
[c]*Mm*: *Mus musculus* (mouse)
[d]*Tb*: *Trypanosoma brucei*

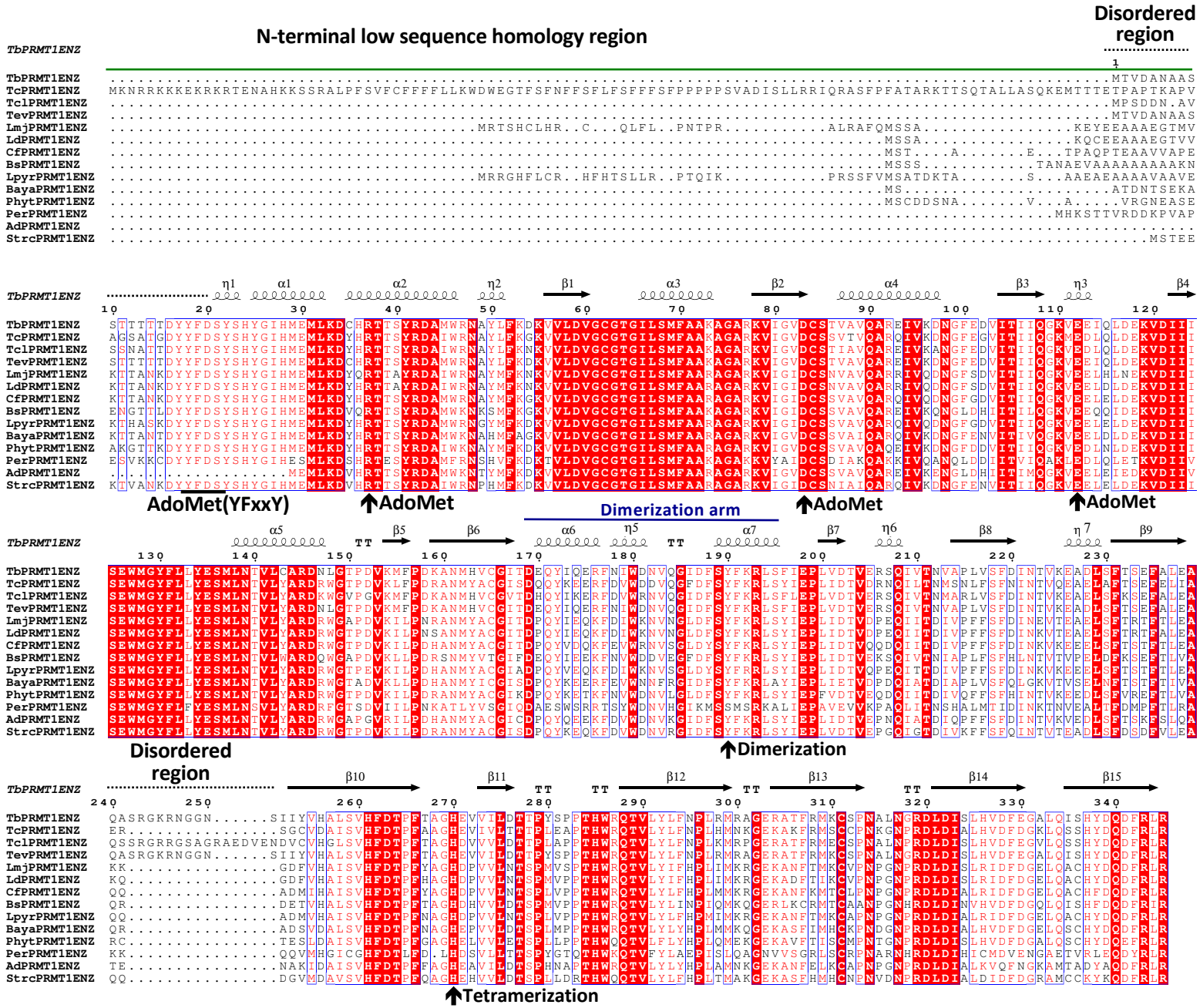

Fig. S1. Multiple sequence alignment of putative PRMT1 enzymes among kinetoplastids. The N-terminal low sequence homology region, secondary structural elements, the dimerization arm, and disordered regions are indicated above the alignment. Key residues for AdoMet binding, dimerization, and tetramerization of *Tb*PRMT1 ENZ are indicated by arrows below the sequence. Tb: *Trypanosoma brucei* (TriTrypDB: Tb927.1.4690), Tc: *Trypanosoma cruzi* (TriTrypDB ID: TcCLB.506529.50), Tcl: *Trypanosoma congolense* (TriTrypDB ID: TcIL3000_1_1890), Tev: *Trypanosoma evansi* (TriTrypDB ID: TevSTIB805.1.4590), *Leishmania major* (TriTrypDB ID: LmjF.12.1270), Ld: *Leishmania donovani* (TriTrypDB ID: LdBPK_120850.1), Cf: *Crithidia fasciculata* (TriTrypDB ID: CFAC1_010018100), Bs: *Bodo saltans* (GenBank ID: CUG92929.1), Lpyr: *Leptomonas pyrrhocoris* (TriTrypDB ID: LpyrH10_23_0130), Baya: *Blechomonas ayalai* (TriTrypDB ID: Baya_031_0090), Per: *Perkinsela sp.* (GenBank ID: KNH05275.1), Ad: *Angomonas deanei* (GenBank ID: EPY25076.1), and Strc: *Strigomonas culicis* (GenBank ID: EPY24636.1).

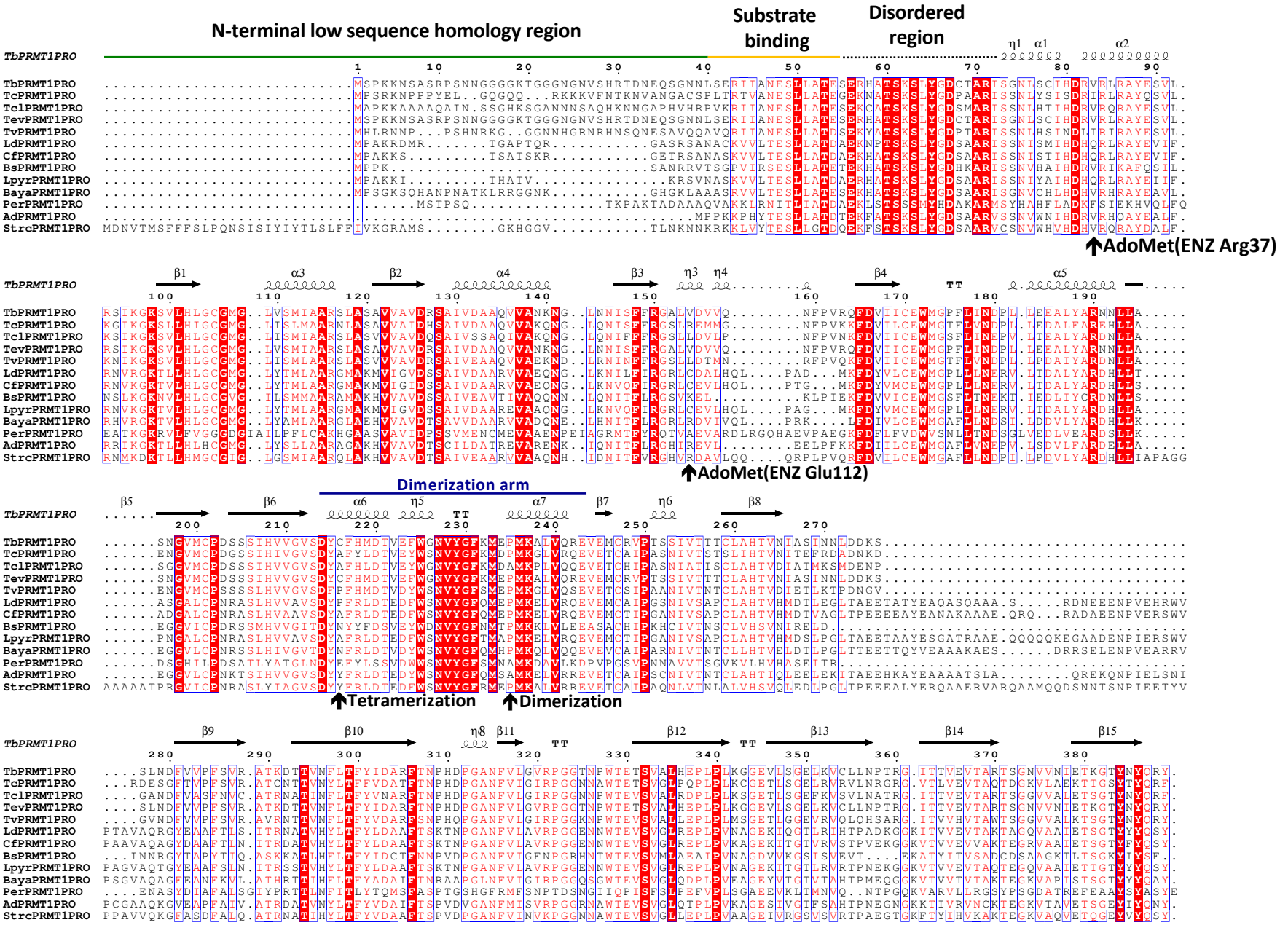

Fig. S2. Sequence alignment of putative PRMT1 prozymes among kinetoplastids. Secondary structural elements, the N-terminal low sequence homology region, the substrate binding region, and the disordered region are indicated above the alignment. Key residues for dimerization, tetramerization, and lack of AdoMet binding residues of *Tb*PRMT1 PRO are indicated by arrows below the sequence. Tb: *Trypanosoma brucei* (TriTrypDB: Tb927.10.3560), Tc: *Trypanosoma cruzi* (TriTrypDB ID: TcCLB.510311.140), Tcl: *Trypanosoma congolense* (TriTrypDB ID: TcIL3000_10_2970), Tev: *Trypanosoma evansi* (TriTrypDB ID: TevSTIB805.10.3790), *Trypanosoma vivax* (TriTrypDB ID: TvY486_1003550), Ld: *Leishmania donovani* (TriTrypDB ID: LdBPK_030580.1), Cf: *Crithidia fasciculata* (TriTrypDB ID: CFAC1_060012600), Bs: *Bodo saltans* (GenBank ID: CUG88155.1), Lpyr: *Leptomonas pyrrhocoris* (TriTrypDB ID: LpyrH10_34_0780), Baya: *Blechomonas ayalai* (TriTrypDB ID: Baya_055_0080), Per: *Perkinsela sp.* (GenBank ID: KNH01754.1), Ad: *Angomonas deanei* (GenBank ID: EPY40540.1), and Strc: *Strigomonas culicis* (GenBank ID: EPY28765.1).

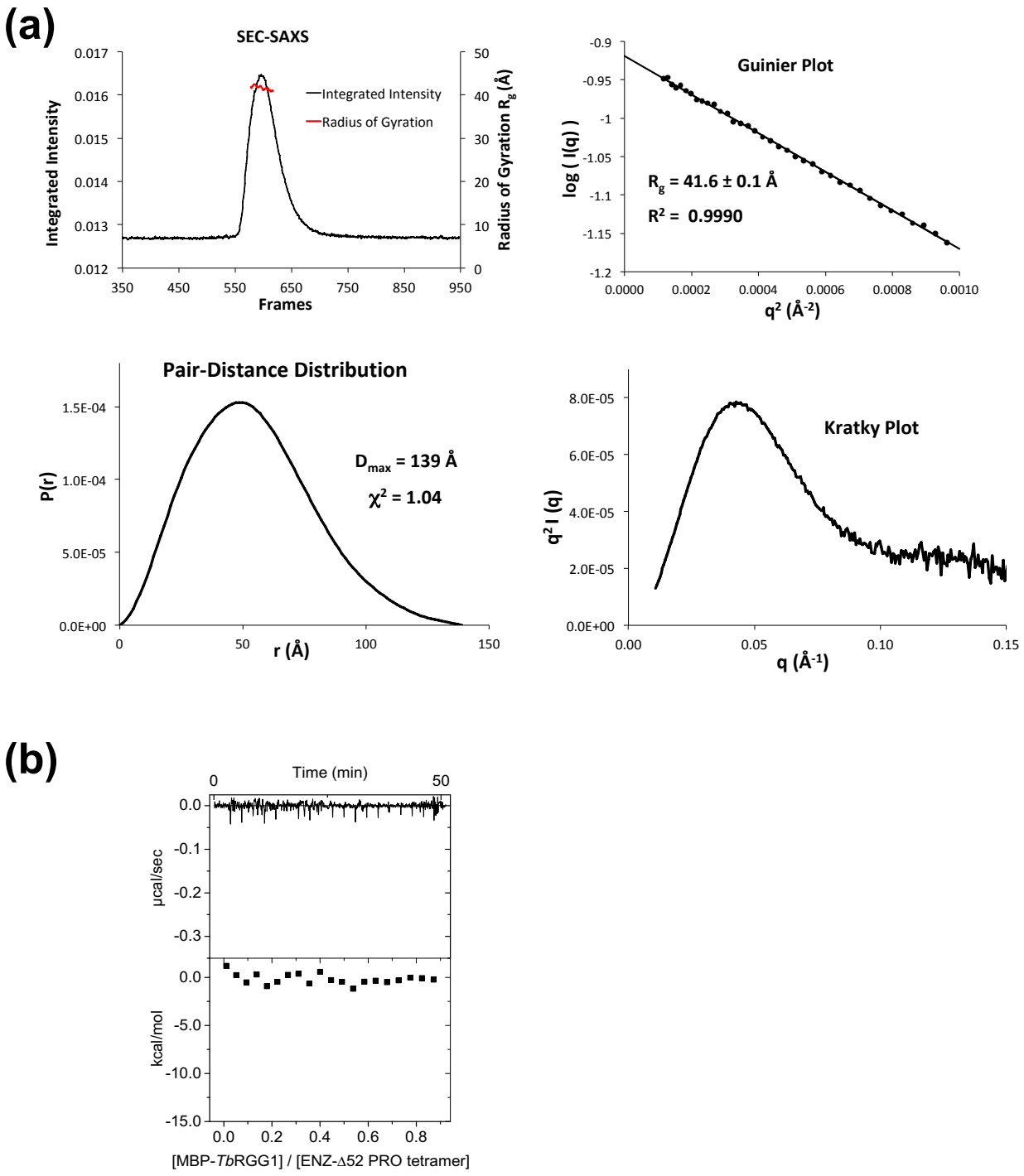

Fig. S3. *Tb*PRMT1 ENZ-Δ52PRO forms a tetramer in solution, but does not bind substrate. (a) Small-angle x-ray scattering analysis. Upper left: SEC-SAXS profile (integrated intensity vs. frames). The red dots indicate R_g values (on the right y-axis) corresponding to frames. Upper right: Guinier plot. Lower left: pair-distance distribution. Lower right: Kratky plot. **(b)** ITC analysis of *Tb*PRMT1 ENZ-Δ52PRO titrated with MBP-*Tb*RGG1.

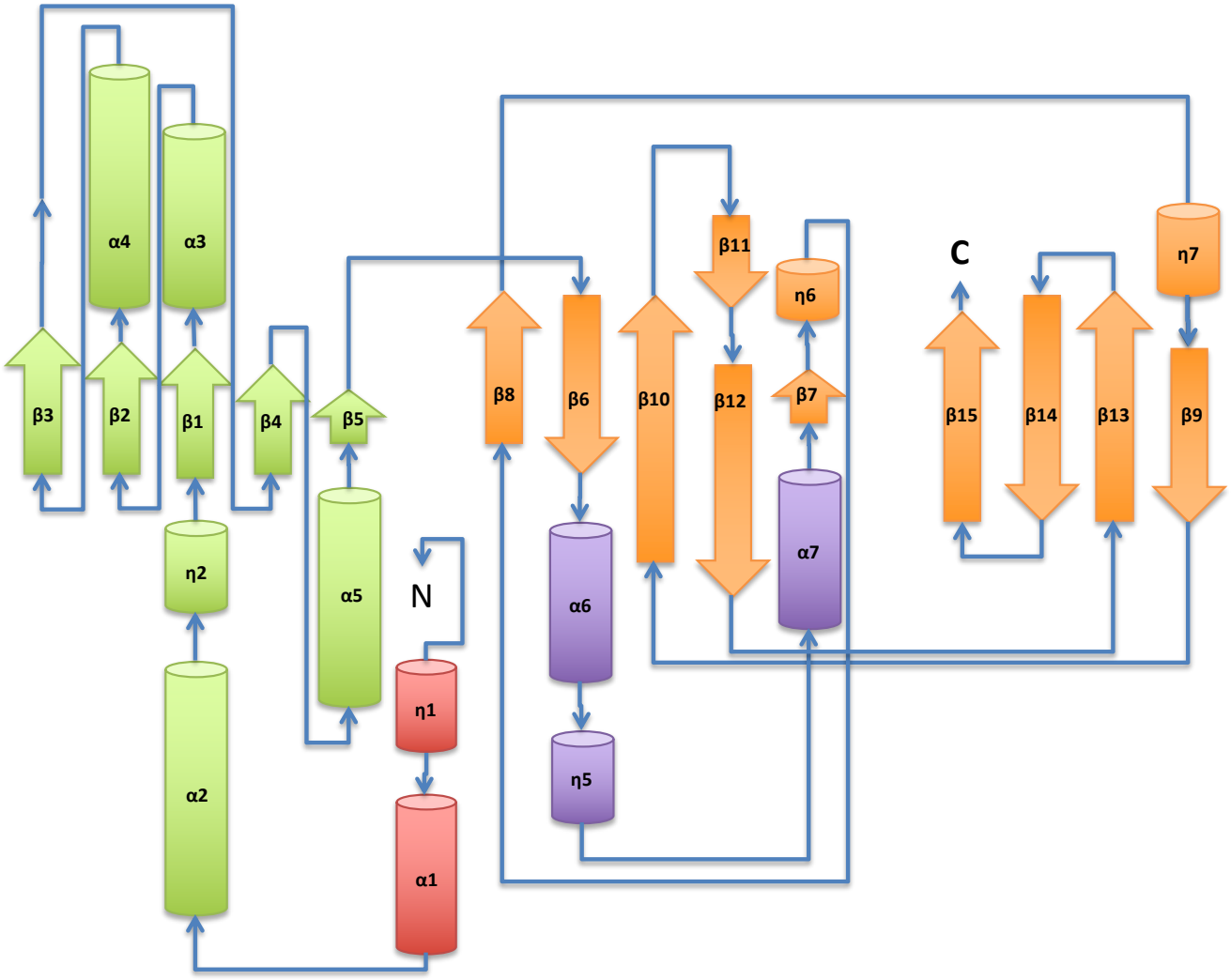

Fig. S4. Topology of *Rattus norvegicus* PRMT1 (PDB: 1OR8).

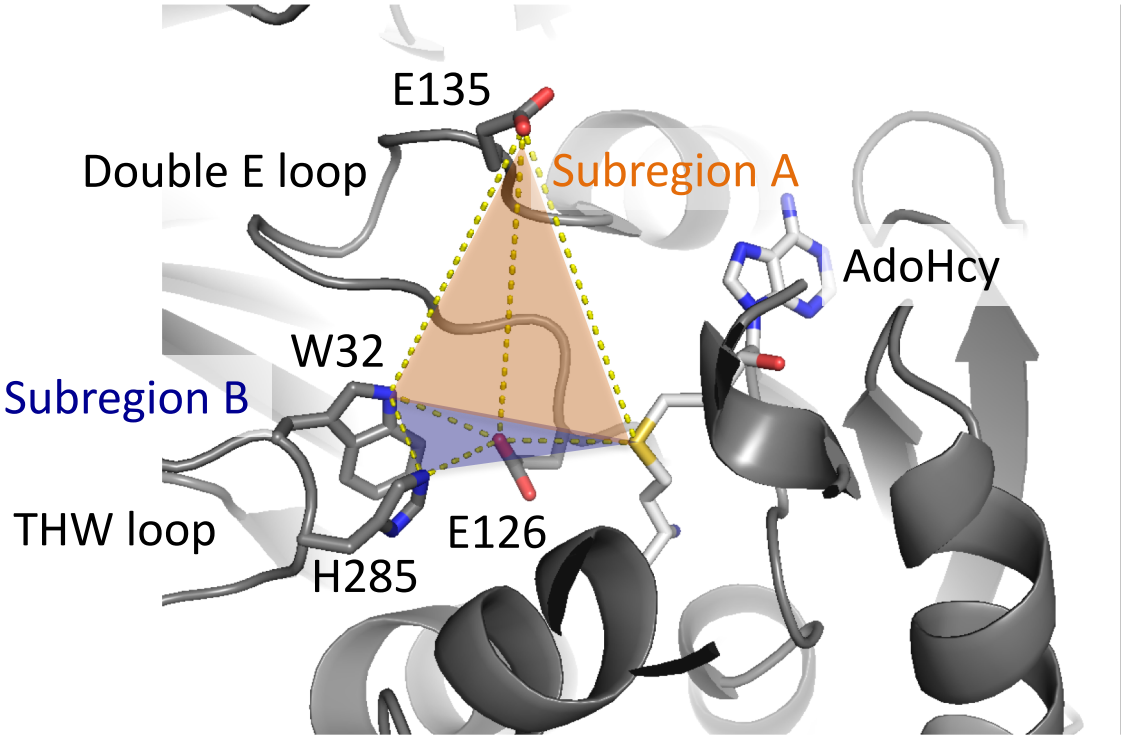

Fig. S5. *Tb*PRMT1 ENZ features a PRMT type I active-site architecture.

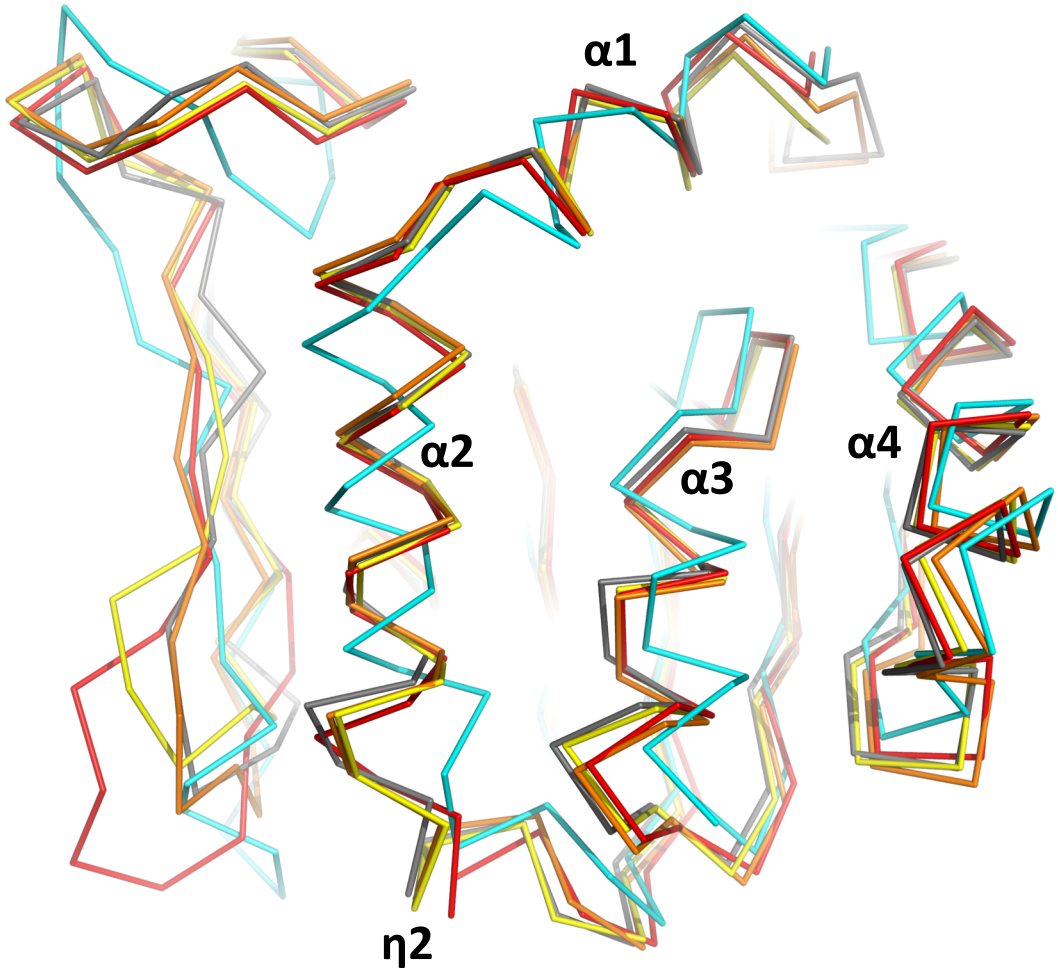

Fig. S6. Superimposition of the Rossmann fold of various PRMT proteins. *Tb*: *Trypanosoma brucei*, *Rn*: *Rattus norvegicus*, *Sc*: *Saccharomyces cerevisiae*.

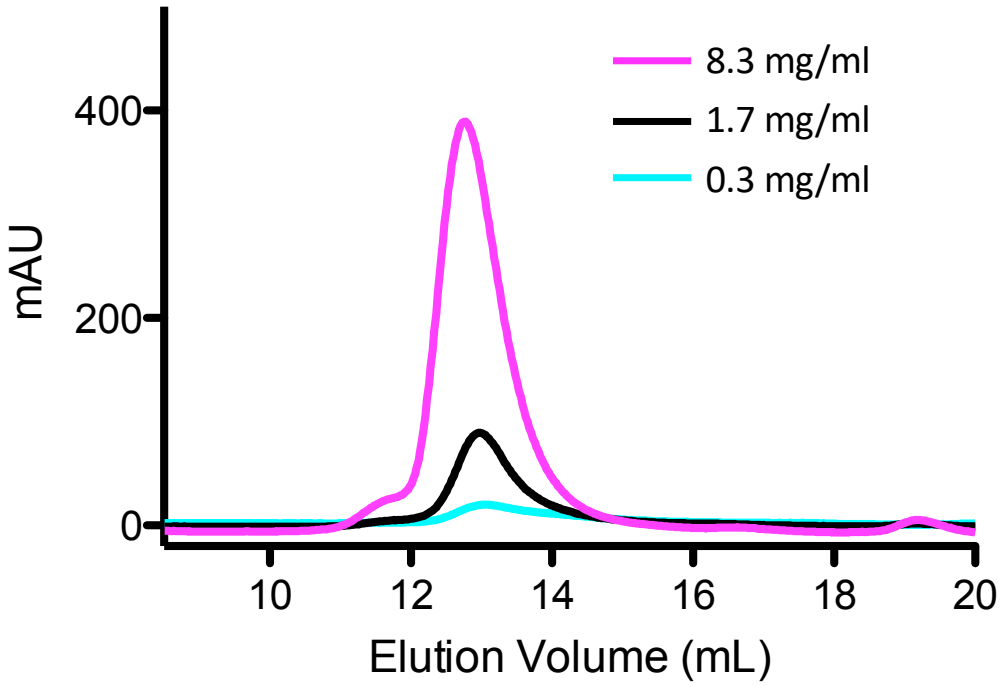

Fig. S7. Concentration-independent heterotetramerization of *Tb*PRMT1 ENZ-PRO. Size-exclusion chromatography (Superdex 200 10/300 column; GE Healthcare) profiles of *Tb*PRMT1 ENZ-PRO at different concentrations. Absorbance was recorded at 280 nm.